

# Gravitational lensing statistics with extragalactic surveys

## IV. Joint constraints from gravitational lensing statistics and CMB anisotropies

Juan Francisco Macias-Perez<sup>1</sup>, Phillip Helbig<sup>1,2</sup>, Ralf Quast<sup>3</sup>, Althea Wilkinson<sup>1</sup>, and Rod Davies<sup>1</sup>

<sup>1</sup> University of Manchester, Jodrell Bank Observatory, Macclesfield, Cheshire SK11 9DL, UK

<sup>2</sup> University of Groningen, Kapteyn Astronomical Institute, P. O. Box 800, 9700 AV Groningen, The Netherlands

<sup>3</sup> University of Hamburg, Hamburg Observatory, Gojenbergsweg 112, 21029 Hamburg, Germany

03 June 1999 / Accepted 21 October 1999

**Abstract.** We present constraints on the cosmological constant  $\lambda_0$  and the density parameter  $\Omega_0$  from joint constraints from the analyses of gravitational lensing statistics of the Jodrell Bank-VLA Astrometric Survey (JVAS), optical gravitational lens surveys from the literature and CMB anisotropies. This is the first time that quantitative joint constraints involving lensing statistics and CMB anisotropies have been presented. Within the assumptions made, we achieve very tight constraints on both  $\lambda_0$  and  $\Omega_0$ . These assumptions are cold dark matter models, no tensor components, no reionisation, CMB temperature  $T_{\text{CMB}} = 2.728$ , number of neutrinos  $n_\nu = 3$ , helium abundance  $Y_{\text{He}} = 0.246$ , spectral index  $n_s = 1.0$ , Hubble constant  $H_0 = 68 \text{ kms}^{-1} \text{ Mpc}^{-1}$ , baryonic density  $\Omega_b = 0.05$ . All models were normalised to the *COBE* data and no closed models ( $k = +1$ ) were computed. Using the CMB data alone, the best-fit model has  $\lambda_0 = 0.60$  and  $\Omega_0 = 0.34$  and at 99% confidence the lower limit on  $\lambda_0 + \Omega_0$  is 0.8. Including constraints from gravitational lensing statistics doesn't change this significantly, although it does change the allowed region of parameter space. A universe with  $\lambda_0 = 0$  is ruled out for any value of  $\Omega_0$  at better than 99% confidence using the CMB alone. Combined with constraints from lensing statistics,  $\lambda_0 = 0$  is also ruled out at better than 99% confidence.

As the region of parameter space allowed by the CMB is, within our assumptions, much smaller than that allowed by lensing statistics, the main result of combining the two is to change the range of parameter space allowed by the CMB along its axis of degeneracy.

**Key words:** gravitational lensing – cosmic microwave background – cosmology: theory – cosmology: observations

### 1. Introduction

Cosmological tests which are sensitive to  $\lambda_0$  and  $\Omega_0$  (the normalised cosmological constant and density parameter, respectively) can be used to construct likelihood contours in the  $\lambda_0$ - $\Omega_0$  plane. Each test usually has a degeneracy such that moving along a curve (which often approximates a line) in the  $\lambda_0$ - $\Omega_0$  plane leaves the likelihood (almost) unchanged. It has long been realised (e.g. Eisenstein et al., 1999a,b) that the direction of degeneracy of constraints from cosmic microwave background anisotropies is roughly orthogonal to that of most other tests. Thus, combining the constraints from CMB anisotropies with those from other cosmological tests can give much tighter constraints than either alone.

Gravitational lensing statistics provide constraints which are degenerate such that  $\lambda_0$  and  $\Omega_0$  values are positively correlated. This is also the case with cosmological tests such as the product of the Hubble constant and the age of the universe, the angular size-redshift (standard rod) test and the luminosity-redshift (standard candle) test. The opposite is the case with constraints derived from CMB anisotropies. Thus, it seems natural to combine the constraints from Quast & Helbig (1999, hereafter Paper I) and Helbig et al. (1999, hereafter Paper II) with an analysis of the type performed by Lineweaver (1998, hereafter L98), which in itself already provides quite tight constraints.

It is important to note that all three of our analyses have fixed all parameters except  $\lambda_0$  and  $\Omega_0$  (though in Papers I and II an attempt has been made to estimate the effect of the uncertainty of the other parameters on the derived constraints on  $\lambda_0$  and  $\Omega_0$  by varying one parameter by two standard deviations (see Paper I)). Ideally, an investigation such as the present one should incorporate the uncertainties in all input parameters into the analysis. Such a programme is currently under development.

In this work, we use the most recent CMB data available to do an analysis similar to that of L98 and combine the constraints with the lensing statistics constraints from Papers I and II following the procedure outlined in Helbig (1999, hereafter Paper III). The plan of this paper is as

---

Send offprint requests to: P. Helbig

Correspondence to: p.helbig@jb.man.ac.uk

follows. In Sect. 2 we describe the procedure used to calculate likelihoods in the  $\lambda_0$ - $\Omega_0$  plane from CMB data and in Sect. 3 we discuss our results and compare them with those from Papers I and II. Sect. 4 summarises our conclusions. For a comparison with other recent constraints from a variety of cosmological tests, see Paper I.

Throughout, as in Papers I, II and III,  $\lambda_0 = \Lambda/3H_0^2$  and  $\Omega_0 = 8\pi G\rho_0/3H_0^2$  refers to the density of matter, i.e. not some ‘total density’ which in our notation would be  $\lambda_0 + \Omega_0$  (or perhaps including a contribution from pressure as well, which we consider to be irrelevant here). The index 0 refers to present-day values, since in general these quantities are time-dependent. (See Paper I for an overview of the rest of our notation and general description of the gravitational lensing statistics method.)

## 2. Constraints from CMB anisotropies

Gravitational lensing statistics are not very sensitive to  $\Omega_0$ . However, CMB data can constrain  $\Omega_0$  more effectively (L98). Following Lineweaver et al. (1997, hereafter L97) we have calculated probability contours in the  $\lambda_0$ - $\Omega_0$  plane. This method is based on a  $\chi^2$  minimisation:

$$\chi^2(\lambda_{0,i}, \Omega_{0,i}) = \sum_{i=1}^{N_{\text{exp}}} \frac{(\text{model}_i(\lambda_{0,i}, \Omega_{0,i}) - \text{temp}_i)^2}{\sigma_i^2} \quad (1)$$

where  $N_{\text{exp}}$  is the number of experiments,  $\text{model}_i$  is the theoretical predicted fluctuation at the multipole range covered by the  $i$ -th experiment and  $\text{temp}_i$  represents the sky fluctuation temperature measured by the  $i$ -th CMB experiment. Each pair  $\lambda_{0,i}, \Omega_{0,i}$  in the  $\lambda_0$ - $\Omega_0$  plane corresponds to a model. We constructed a matrix of models and calculated the  $\chi^2$  and the likelihood associated with it,  $e^{-\frac{\chi^2}{2}}$ . The theoretical power spectra were calculated with the help of CMBFAST<sup>1</sup> (Zaldarriaga, 1998). The models depend on a range of parameters. To make the test computationally feasible, we fixed all of them except  $\Omega_0$  and  $\lambda_0$ . We consider cold dark matter models, no tensor components and no reionisation. No closed models ( $k = +1$ ) were computed because CMBFAST does not yet support this (we are looking forward to the new CMBFAST version which will include these models). The CMB temperature was set to  $T_{\text{CMB}} = 2.728$ , the number of neutrinos to  $n_\nu = 3$  and the helium abundance to  $Y_{\text{He}} = 0.246$ . The spectral index used was  $n_s = 1.0$ . All models were normalised to the *COBE* data.<sup>2</sup> Finally, the Hubble constant and the baryonic density were set to  $H_0 = 68 \text{ km s}^{-1} \text{ Mpc}^{-1}$  and  $\Omega_b = 0.05$ . All these values were based on the best literature estimates and on the L98 conclusions.  $\lambda_0$  and  $\Omega_0$  vary in the range  $-0.48 \leq \lambda_0 \leq 1.48$  and  $0.06 \leq \Omega_0 \leq 0.98$  with a resolution of 0.04.  $\Omega_0 = 0.02$  models were not computed since this is inconsistent with our value for  $\Omega_b$ ; these models, and all outside the examined parameter space, were

assigned an a priori likelihood of zero. Otherwise, we have used a uniform prior. (See Paper I for further discussion.) (Note that this is smaller than the range of parameter space covered in Papers I and II, but with a finer resolution. Initially, we explored the parameter space as follows:  $\lambda_0$  and  $\Omega_0$  vary in the range  $-3 \leq \lambda_0 \leq 1$  and  $0.1 \leq \Omega_0 \leq 1.5$  with a resolution of 0.1, slightly smaller than the range of parameter space covered in Papers I and II but with the same resolution. We restricted ourself to the higher resolution calculations in the smaller area of parameters space as outside of this no significant likelihood is present.)

To compare data and models, the models have to be convolved with the window function of the CMB experiments. The window function delimits the multipole range to which the experiment is sensitive. This can be seen as a Fourier transform of the experimental beam function in the multipole space (White & Srednicki, 1995). On the other hand, to compare results from different CMB experiments, the effect of the window function must be removed. This is accomplished by deconvolving both the model and the data (see L97 for more details). The quantities  $\text{model}_i$  and  $\text{temp}_i$  are the deconvolved values.

We have built up a CMB data compilation that is based on L98 and on the web page provided by Tegmark.<sup>3</sup> We have also added new data from the Tenerife radiometers and interferometer (Dicker et al., 1999). A list of the data used with their references can be found in Table 1. The window functions of each of the experiments have been also gathered. We have calculated some of them from analytical expressions (White & Srednicki, 1995). The rest can be found in each of the CMB experiment web pages which can be accessed from Tegmark’s web page mentioned at the start of this paragraph.

We do not actually use the COBE points from Tegmark & Hamilton (1997), since the COBE data are used internally by CMBFAST. We include them in Table 1 since they appear in Fig. 5. On the one hand, CMBFAST normalises the power spectra to COBE according to the fitting formula given in Bunn & White (1997). In order to take into account the *shape* of the power spectrum in the region of the COBE data, as well as its *amplitude*, we have multiplied the likelihood obtained from our  $\chi^2$  analysis (without the COBE points) with the likelihood (again provided by CMBFAST using a formula from Bunn & White (1997)) of the corresponding power spectra relative to a flat power spectrum.

## 3. Results

### 3.1. CMB results

Fig. 1 shows the likelihood  $e^{-\frac{\chi^2}{2}}$  obtained from the  $\chi^2$  calculations over our matrix of cosmological models, for

<sup>1</sup> <http://www.sns.ias.edu/~matiasz/CMBFAST/cmbfast.html>

<sup>2</sup> See the last paragraph of this section.

<sup>3</sup> <http://www.sns.ias.edu/~max/cmb/experiments.html>

**Table 1.** CMB data used. The window function is centered at  $l = l_{\text{eff}}$  and drops to half of its central value at  $l_{\text{min}}$  and  $l_{\text{max}}$ , except for COBE, where  $l_{\text{min}}$  and  $l_{\text{max}}$  instead indicate the RMS width of the window function. The COBE points from Tegmark & Hamilton (1997) are not actually used in our  $\chi^2$  analysis, but are included here since they appear in Fig. 5; see text for details

Experiment	$\delta T$ ( $\mu\text{K}$ )	+	-	$l_{\text{min}}$	$l_{\text{eff}}$	$l_{\text{max}}$	Reference
COBE 1	8.5	16.0	8.5	2	2.1	2.5	Tegmark & Hamilton (1997)
COBE 2	28.0	7.4	10.4	2.5	3.1	3.7	Tegmark & Hamilton (1997)
COBE 3	34.0	5.9	7.2	3.4	4.1	4.8	Tegmark & Hamilton (1997)
COBE 4	25.1	5.2	6.6	4.7	5.6	6.6	Tegmark & Hamilton (1997)
COBE 5	29.4	3.6	4.1	6.8	8.0	9.3	Tegmark & Hamilton (1997)
COBE 6	27.7	3.9	4.5	9.7	10.9	12.2	Tegmark & Hamilton (1997)
COBE 7	26.1	4.4	5.3	12.8	14.3	15.7	Tegmark & Hamilton (1997)
COBE 8	33.0	4.6	5.4	16.6	19.4	22.1	Tegmark & Hamilton (1997)
FIRS	29.4	7.8	7.7	3.0	10	30.0	Ganga et al. (1994)
Tenerife	32.5	10.1	8.5	13	20	31	Hancock et al. (1997)
SP	32.21	7.44	4.08	31	57	106	Gundersen et al. (1995)
BAM	55.6	27.4	9.8	28	74	97	Tucker et al. (1997)
ARGO	42.01	6.41	7.06	52	95	176	de Bernardis et al. (1994)
MAX	43.44	7.24	4.94	78	145	263	Tanaka et al. (1996)
Python 1	54.0	14.0	12.0	68	92	129	Platt et al. (1997)
Python 2	58.0	15.0	13.0	119	177	243	Platt et al. (1997)
IAC/Bartol	55.0	27.0	22.0	35	53	79	Femenia et al. (1998)
MSAM1	48.42	11.95	7.95	86	160	251	Cheng et al. (1996)
MSAM2	59.34	12.08	8.23	173	263	383	Cheng et al. (1996)
QMAP F1 Ka	49.0	6.0	7.0	47	92	157	Devlin et al. (1998)
QMAP F1 Q	47.0	8.0	10.0	38	84	140	Devlin et al. (1998)
QMAP F2 Ka	46.0	10.0	12.0	44	91	138	Herbig et al. (1998)
QMAP F2 Ka	63.0	10.0	12.0	81	145	209	Herbig et al. (1998)
QMAP F2 Q	56.0	5.0	6.0	58	125	192	Herbig et al. (1998)
QMAP F1+2 Ka	47.0	6.0	7.0	39	80	121	de Oliveira-Costa et al. (1998)
QMAP F1+2 Ka	59.0	6.0	7.0	72	126	180	de Oliveira-Costa et al. (1998)
QMAP F1+2 Q	52.0	5.0	5.0	47	111	175	de Oliveira-Costa et al. (1998)
Saskatoon 1	49.0	8.0	5.0	53	86	132	Netterfield et al. (1997)
Saskatoon 2	69.0	7.0	6.0	119	166	206	Netterfield et al. (1997)
Saskatoon 3	85.0	10.0	8.0	190	236	274	Netterfield et al. (1997)
Saskatoon 4	86.0	12.0	10.0	243	285	320	Netterfield et al. (1997)
Saskatoon 5	69.0	19.0	28.0	304	348	401	Netterfield et al. (1997)
CAT 1	48.44	7.67	5.71	339	422	483	Scott et al. (1996)
CAT 2	45.20	11.02	8.13	546	610	722	Scott et al. (1996)
RING5M 2	56.0	8.5	6.6	361	589	756	Leitch et al. (1999)

the CMB data. The contours correspond to 68%, 90%, 95% and 99% confidence levels, i.e. the area within the  $x\%$  contour level contains  $x\%$  of the sum of all the likelihood values (one per pixel) in the plot. (See Paper III for further discussion of this point, which is important for the detailed comparison of different results in the literature.) These confidence limits differ from those used in L98 in two ways. First, we plot the  $x\%$  contour as that which encloses  $x\%$  of the integrated probability density in the  $\lambda_0$ - $\Omega_0$  plane, i.e. joint probability contours in  $\lambda_0$  and  $\Omega_0$ , whereas those in L98 correspond to the appropriate confidence levels *when projected onto one of the axes*. Thus, our contours are naturally larger than those of L98. Second, the contours of L98 are actually  $\Delta\chi^2$  contours, which correspond to the appropriate confidence intervals if Gaussianity is assumed, whereas ours are ‘real’ confidence contours as defined above. (See Papers I and III for further discussion.)

It is well known that the errors quoted for CMB temperature fluctuation measurements are not Gaussian. Actually, for most of the experiments the error bars quoted are asymmetric. The observational temperature fluctuations are usually calculated using maximum likelihood techniques, with the value corresponding to the mean and the error to the  $1\text{-}\sigma$  cutoff. We have taken asymmetric error bars into account by using the positive or negative error bar according to whether the theoretical value falls above or below the experimental value. There is perhaps some disagreement as to the errors that the assumption of Gaussianity introduces on the constraints on  $\lambda_0$  and  $\Omega_0$ . The L98 confident limits are based on the  $\chi^2$  method, which assumes that the likelihood function is a Gaussian. Other groups (e.g. Bartlett et al., 1998a,b, 1999a,b) consider this approximation to be not justified and base their calculations on *likelihood functions*. Unfortunately, likelihood functions are not provided for all the CMB experi-

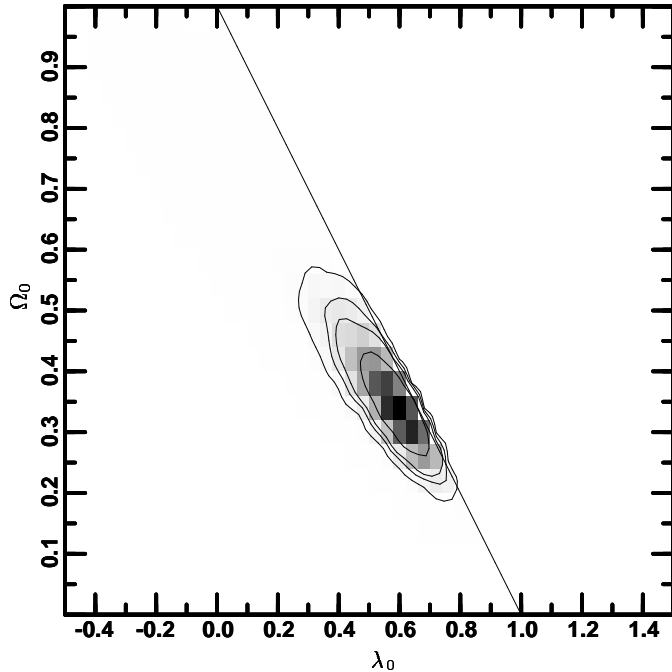


**Fig. 1.** The likelihood function  $p(D|\lambda_0, \Omega_0, \xi_0)$  based on the CMB data in Table 1. ( $\xi_0$  represents the parameters other than  $\lambda_0$  and  $\Omega_0$ ;  $\xi_0$ , which corresponds to ‘nuisance parameters’, was held constant for all calculations in this paper. See Quast & Helbig (1999, Paper I) for definitions and further discussion.) All nuisance parameters are assumed to precisely take their mean values. The pixel grey level is directly proportional to the likelihood ratio, darker pixels reflect higher ratios. In this and all subsequent plots, unless noted otherwise, the pixel size reflects the resolution of our numerical computations, the contours mark the boundaries of the minimum 0.68, 0.90, 0.95 and 0.99 confidence regions for the parameters  $\lambda_0$  and  $\Omega_0$  and are ‘real contours’ in the sense of the discussion in Helbig (1999, Paper III). The diagonal line corresponds to  $k = 0$ ; the area to the right of this corresponds to spatially closed models which were not examined here. The fact that some grey pixels and contours are nevertheless in this region is due to finite resolution and interpolation, respectively

ments and their calculations are based on approximations. How to compute this approximation is still poorly understood. We have opted for a much simpler approach by using the likelihood defined above instead of the confidence limits provided by the  $\chi^2$  statistics. Contours using the maximum likelihood approach seem to be larger than those from Gaussian statistics. Our contours are found to lie between the approach of L97 and L98 and that of Bartlett et al. (1998b, 1999a).<sup>4</sup>

<sup>4</sup> ‘Gaussianity’ is an issue in at least three different contexts with relation to cosmological constraints derived from CMB anisotropies. First, the correspondence between  $\Delta\chi^2$  values or fractions of the peak likelihood and ‘real’ confidence contours as defined above often assumes Gaussianity. Second, not unrelated, there is the issue of the Gaussianity of the error bars

### 3.2. Review of lens statistics results

We have repeated the lens statistics calculations of Papers I and II at the higher resolution ( $\Delta\lambda_0 = \Delta\Omega_0 = 0.04$ ) and in the area ( $-0.48 \leq \lambda_0 \leq 1.48$  and  $0.02 \leq \Omega_0 \leq 0.98$ ) used in the CMB calculations. For comparison with Papers I and II, these are shown in Fig. 2.

### 3.3. Joint constraints

We follow the procedure outlined in Paper III in computing joint constraints. First, to make sure that the cosmological tests are not inconsistent with each other, we plot the overlap of various contours in Fig. 3. In Fig. 4, we present joint constraints formed by the multiplication of the corresponding probability density functions. There is (at least a small) region of overlap between the CMB contour and *all* the lensing statistics contours at 90% confidence (and of course at 95% and 99% as well), and with the JVAS contour (which we consider to be more reliable than the optical or joint contours) at 68% confidence. Thus, we consider the CMB and lensing constraints to be consistent or, at worse, only marginally inconsistent.

Note that the joint constraints using lensing statistics and the CMB data differ only slightly from those using the CMB data alone. (It should be remembered that both the CMB and the lensing constraints are probably too tight since all parameters (except of course  $\lambda_0$  and  $\Omega_0$ ) have been fixed for this analysis. With more and better data, both can be expected to improve in the future, while improvements in the theoretical models will reduce systematic effects. However, since the input parameters to the lensing statistics analysis are in many cases better understood than those for the CMB analysis, the lensing statistics constraints are probably more realistic than those from the CMB. One should thus not conclude that the CMB constraints make lensing statistics superfluous.) Nevertheless, the addition of even the current lens statistics data tightens the upper limit on  $\lambda_0$  and the lower limit on  $\Omega_0$ . While the CMB data alone provide perhaps the tightest constraints (with the above-mentioned caveats) of any cosmological test, they still allow an area of parameter space which is ruled out by other cosmological tests, among which are lensing statistics. Not only the upper (lower) limit on  $\lambda_0$  ( $\Omega_0$ ) is tightened by adding lens statistics constraints to those from the CMB, but also the best-fit cosmological model shifts to a lower  $\lambda_0$  and higher  $\Omega_0$  value.

The degeneracy in the  $\lambda_0$ - $\Omega_0$  plane is such that, in the region of non-negligible likelihood, the constraints from the CMB alone as well as the joint constraints with lensing statistics measure approximately  $\lambda_0 + \Omega_0$ . This region is described by the 99% confidence contour, which covers

---

of individual experiments. Third is the question whether the primordial density fluctuations are Gaussian.

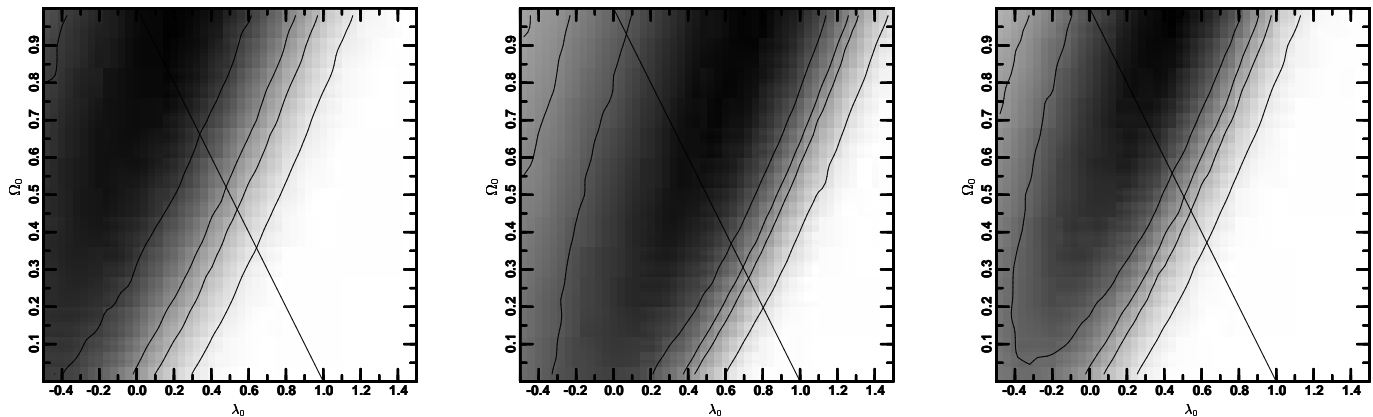


**Fig. 2.** *Left:* The likelihood function  $p(D|\lambda_0, \Omega_0)$  from optical gravitational lens surveys discussed in Quast & Helbig (1999, Paper I), but with a higher resolution and confined to a smaller area of parameter space. (This makes the positions of the contours slightly different; see Helbig (1999, Paper III) for a discussion.) *Centre:* The same but from the analysis of JVAS presented in Helbig et al. (1999, Paper II). *Right:* The same but joint constraints from the two other plots as discussed in Paper II

the range in  $\lambda_0$  of 0.3–0.8 for the CMB alone. In the case of joint constraints, the region is shifted to lower  $\lambda_0$  values as well as slightly increased in size, the exact values depending on the (combination of) lensing constraints used. The corresponding range for  $\Omega_0$  is 0.18–0.57, with a similar shifting to higher  $\Omega_0$  values (and increase in range) for the joint constraints. (Of course, the 99% confidence contour is smaller than the rectangle defined by the ranges of  $\lambda_0$  and  $\Omega_0$ .)

Taken together, present measurements of cosmological parameters *definitely* rule out the Einstein-de Sitter universe ( $\lambda_0 = 0, \Omega_0 = 1$ ), *very probably* rule out a universe without a cosmological constant ( $\lambda_0 = 0$ ) and *tentatively* rule out a flat ( $\lambda_0 + \Omega_0 = 1$ ) universe as well.<sup>5</sup> A universe with  $\lambda_0 \approx 0.4$  and  $\Omega_0 \approx 0.3$  seems to be consistent with all observational data, including measurements of the Hubble constant and age of the universe. It should be noted that it is really only the CMB data which are indicating a possibly non-flat universe. Other combinations of cosmological tests (e.g. Roos & Harun-or-Rashid, 1999; Turner, 1999, and references therein) tend to allow a flat universe within the errors.

The  $\chi^2$  minimum for the CMB data is obtained for  $\Omega_0 = 0.34$  and  $\lambda_0 = 0.60$ . The power spectrum (with the data points) for this best-fit model is shown in the solid curve in Fig. 5. This is also the best-fit model when the CMB constraints are combined with those from JVAS as in the centre plot of Fig. 4. The best-fit model for the combination of CMB and optical lensing constraints, either with or without the addition of JVAS constraints,

<sup>5</sup> This *tentative* conclusion should be considered with the necessary caution. Apart from caveats arising from the limited parameter space explored (i.e. all nuisance parameters were fixed), the confidence contours cannot be interpreted straightforwardly due to the fact that no closed models were computed.

has  $\Omega_0 = 0.38$  and  $\lambda_0 = 0.52$ ; this is shown in the dashed curve of Fig. 5.

The comparison values from this work corresponding to those in Table 3 of Paper I are presented in Table 2.

Holding most of the parameters constant is of course a weak point of our approach. Obviously, the goal is to explore the entire range of parameter space, incorporating uncertainties in all parameters, prior information etc. This is computationally very expensive. Alternatively, we could also think of a multiparameter maximisation method which would provide a ‘best fit’ value for all parameters, although assigning an error would not be straightforward. This might be risky because of possible secondary maxima. In fact, our calculations *do* show a secondary maximum, as can be seen by examining the data mentioned in the URL below, although it is too weak to show up in the plots. The fact that the secondary maximum occurs around  $\lambda_0 = -1$  and  $\Omega_0 = 1$  looks suspicious, but there is nothing obviously wrong with the behaviour of CMBFAST here (M. Zaldarriaga, private communication).<sup>6</sup> This does appear to be ‘real’ in the sense that it is what the comparison of the data with the CMBFAST power spectra indicate. Of course, there might be unknown systematic effects in the former, but as far as we can tell, there are no problems with CMBFAST which could produce this. On the other hand, it is probably not ‘real’ in the sense that it might disappear when more and/or better input data are used or when a more exact code than the current version of CMBFAST—especially for the relatively poorly explored area of parameter space where this secondary maximum occurs—is used. It should be kept in mind, however, that there is no a priori reason to exclude a secondary maximum. Also, this secondary maximum appears in a part of parameter space which is

<sup>6</sup> Initially, we *did* find a bug in CMBFAST for  $\Omega_0 = 1$  and  $\lambda_0 < 0$ , but this has since been corrected.

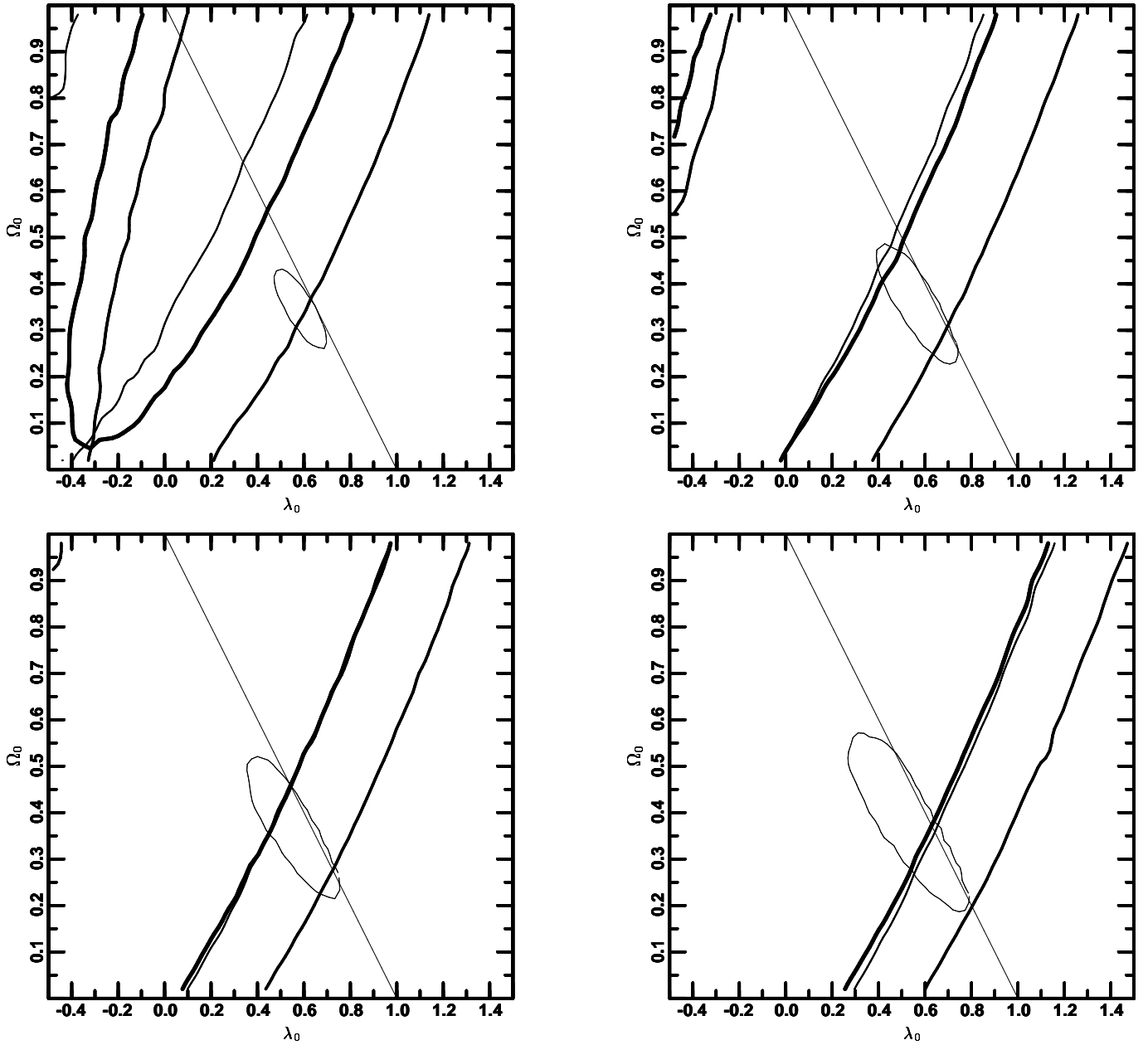


**Fig. 3.** The 68% (top left), 90% (top right), 95% (bottom left) and 99% (bottom right) confidence contours for each of the data sets shown in Figs. 1 and 2. In order of increasing thickness, the curves correspond to Fig. 1 and, from left to right, the plots in Fig. 2

**Table 2.** Mean values and ranges for assorted confidence levels for the parameter  $\lambda_0$  for our likelihoods from this work, for the special case  $\Omega_0 = 0.3$ . This should be compared to Table 3 in Paper I. Only lower limits are given for the case of the CMB alone, as the upper limits all lie in the  $k = +1$  area of parameter space, which was not examined. The contours near the  $k = 0$  line are thus not ‘real’ and should be ignored. Since  $k = +1$  was not examined, no values for the  $k = 0$  case can be extracted, as was the case in the corresponding tables in Papers I and II. However, the  $k = 0$  special case has been examined in detail in L97.  $X$  denotes the fact that there is no intersection of the confidence contour with the  $\Omega_0 = 0.3$  line; equal upper and lower limits indicate a tangency

Cosmological test	68% c.l. range		90% c.l. range		95% c.l. range		99% c.l. range	
CMB, $p(D \lambda_0)$	0.58		0.54		0.52		0.49	
CMB & optical, $p(D \lambda_0)$	0.62	0.62	0.54	0.69	0.52	0.70	0.49	0.72
CMB & JVAS, $p(D \lambda_0)$	0.58	0.69	0.54	0.70	0.52	0.71	0.49	0.72
CMB & optical & JVAS, $p(D \lambda_0)$	$X$	$X$	0.55	0.66	0.52	0.69	0.50	0.71

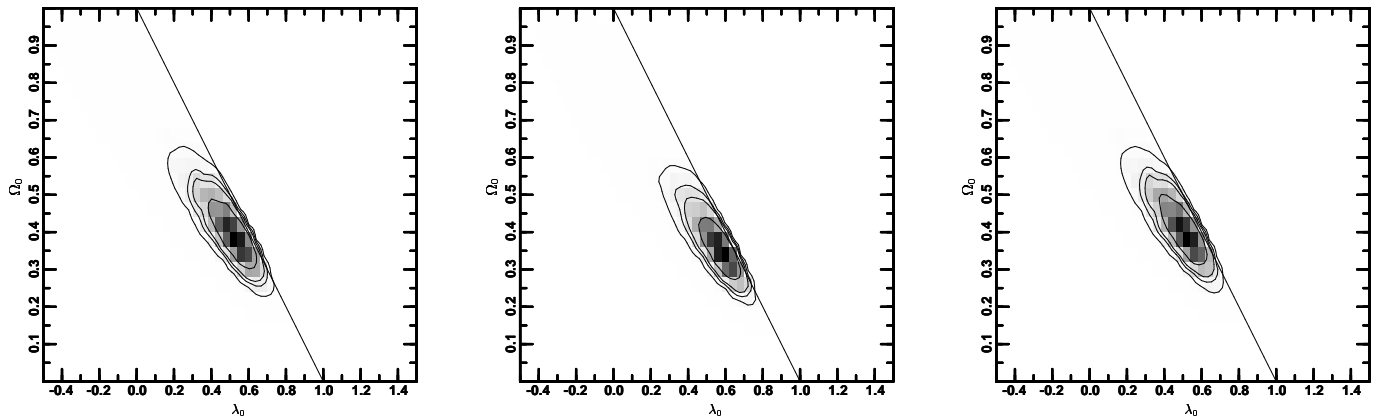


Fig. 4. The same as Fig. 2 but combined with the CMB constraints from Fig. 1

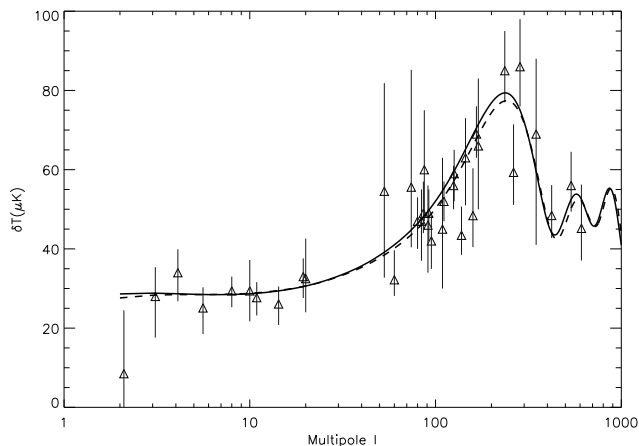


Fig. 5. Data points with error bars and the power spectrum for our best-fit model based on the CMB data alone or, as the values are the same, on the joint constraints from CMB and JVAS (solid) and for the combination of the CMB data with either the optical surveys discussed in Paper I or with both the optical surveys and JVAS (dashed) (again, the values are the same)

ruled out when a few cosmological tests are considered simultaneously (see Paper I), so in that sense it is also probably not ‘real’.

The CMB data alone do not rule out closed ( $k = +1$ ) models (see also White & Scott, 1996). The probability contours are thus compressed near the line that separates the open models from the closed ones. This is due to CMB-FAST not (yet) being able to make calculations for  $k = +1$  models. Even if these can be ruled out by (some combination of) other cosmological tests, it would be useful to extend the calculations formed here to include closed models, which would allow for an easier interpretation of joint cosmological constraints which include those from CMB data.

As mentioned in Papers I–III, to aid comparisons with other cosmological tests, the data for the figures shown in this paper are available at

[http://multivac.jb.man.ac.uk:8000/ceres/data\\_from\\_papers/](http://multivac.jb.man.ac.uk:8000/ceres/data_from_papers/)

or

[http://gladia.astro.rug.nl:8000/ceres/data\\_from\\_papers/](http://gladia.astro.rug.nl:8000/ceres/data_from_papers/)

and we urge our colleagues to follow our example.

#### 4. Conclusions

We have performed an analysis similar to that of Line-weaver (1998), but have used slightly different input data and a slightly different statistical technique. We have then combined the constraints in the  $\lambda_0$   $\Omega_0$  derived from the CMB with the results of the constraints from gravitational lensing statistics presented in Quast & Helbig (1999, Paper I) and Helbig et al. (1999, Paper II).

Using the CMB data alone, the best-fit model has  $\lambda_0 = 0.6$  and  $\Omega_0 = 0.34$  and at 95% confidence the lower limit on  $\lambda_0 + \Omega_0$  is 0.8. Including constraints from gravitational lensing statistics doesn’t change this significantly, although it does change the allowed region of parameter space. A universe with  $\lambda_0 = 0$  is ruled out for any value of  $\Omega_0$  at better than 99% confidence using the CMB alone. Combined with constraints from lensing statistics,  $\lambda_0 = 0$  is also ruled out at better than 99% confidence.

As the region of parameter space allowed by the CMB is, within our assumptions, much smaller than that allowed by lensing statistics, the main result of combining the two is to change the range of parameter space allowed by the CMB along its axis of degeneracy. This axis of degeneracy is along a line of constant  $\Omega_0 + \lambda_0$ , i.e. along a line of constant radius of curvature. Indeed, it is close to the  $\Omega_0 + \lambda_0 = 1$  line, which corresponds to a flat universe.

The CMB analysis favours  $\lambda_0 \approx 0.60$  and  $\Omega_0 \approx 0.34$ . This confirms the long-established result that the  $\lambda_0 = 0$ ,

$\Omega_0 = 1$  (Einstein-de Sitter) model is ruled out by the data and supports the recent evidence for a positive cosmological constant (see Papers II and III for a discussion). The combination of results discussed in Paper II and Lineweaver (1998) hinted tentatively that flat ( $k = 0$ ) cosmological models are beginning to be ruled out by the data. However, to quantify this, it would be interesting to compute power spectra for spatially closed ( $k = +1$ ) cosmological models, since these are not ruled out by current CMB data.

One should keep in mind that these conclusions assume fixed values for the nuisance parameters. On the other hand, these fixed values correspond to values which are (currently) generally accepted and/or values at the global  $\chi^2$  minimum in a larger parameter space examined in L98.

On the one hand, the CMB data provide good evidence for a flat universe, since the allowed region of parameter space is very small and very near the  $k = 0$  line. On the other hand, as noted in L98, the allowed region is so small that a significant departure from  $k = 0$  is hinted at. (However, one should keep in mind that either of these might be a consequence of not taking the uncertainties in the other parameters fully into account.) Nevertheless, compared to other cosmological tests which allow a larger portion of the  $\lambda_0$ - $\Omega_0$  plane, the CMB provides a strong hint that the universe is close to being flat. On the other hand, the *combination* of the CMB data and the data from other cosmological tests tend to indicate that the best fit might actually be achieved for  $k < 0$ , as discussed in Paper I. While various tests might individually allow  $k = 0$ , they do so for different values of  $\lambda_0$  (or, equivalently,  $\Omega_0$  which of course is  $1 - \lambda_0$  in a flat universe) so that, in combination, they provide evidence against a flat universe.

If the universe does have  $k = 0$  or is arbitrarily close to it, this can never be proven in practice, though our confidence in a measurement indicating  $k = 0$  would be inversely proportional to the size of the error bars. On the other hand, if the universe is in fact not flat, then this *can* be proven, by reducing the error bars so that the  $k = 0$  case is ruled out. At present, the question of the sign of  $k$  or equivalently (assuming a simple topology) the question whether the universe is finite or infinite is still an open question. On the other hand, there is strong evidence for the fact that it will expand forever.

Assuming the universe is not flat then, since it is relatively close to being so, to demonstrate that it is not flat it will be necessary to reduce the systematic errors in the comparison of observations with theory. This can be done by incorporating the uncertainties in all input parameters into the calculations (for CMB constraints and other cosmological tests). Of course, it is also necessary to explore a large enough region of parameter space, in all dimensions, in sufficient resolution.

While the joint constraints leave only a small area of the  $\lambda_0$ - $\Omega_0$  parameter space which fits the observations, it should be remembered that neither the CMB nor the lens

statistics analyses we have performed incorporates uncertainties in the input parameters: all parameters except  $\lambda_0$  and  $\Omega_0$  have been held constant. This is sensible in a first-step approach, but of course an analysis of the full parameter space should be performed in order to get robust constraints on  $\lambda_0$ ,  $\Omega_0$  and the other parameters these analyses are sensitive to. Our suspicion is that as a result of this the CMB constraints will relax more than the lensing statistics constraints, so, despite the impression that the figures here give that the CMB on its own is powerful enough to constrain the cosmological parameters, one should also include gravitational lensing statistics in 'joint constraints' analyses (e.g. White, 1998; Eisenstein et al., 1999a; Tegmark et al., 1998a,b; Eisenstein et al., 1998; Webster et al., 1998). This will become more important in the future with the completion of large, well-defined gravitational lens surveys such as CLASS (e.g. Myers et al., 1999).

*Acknowledgements.* It is a pleasure to thank D. Barbosa, E. Bunn, G. Hinshaw and C. Lineweaver for helpful discussions and M. Zaldarriaga and U. Seljak for making their CMBFAST code publicly available. This research was supported in part by the European Commission, TMR Programme, Research Network Contract ERBFMRXCT96-0034 'CERES'. JFMP acknowledges the support of a PPARC studentship.

## References

- Banday A.J., Sheth R.K., da Costa L.N. (eds.), 1999, *The Evolution of Large-Scale Structure: From Recombination to Garching*
- Bartlett J.G., Blanchard A., Dour M.L., Douspis M., 1998a, In: Thanh & Giraud-Heraud (1998), astro-ph/9804158
- Bartlett J.G., Blanchard A., Douspis M., Dour M.L., 1998b, In: *The CMB and the Planck Mission*, astro-ph/9810316
- Bartlett J.G., Blanchard A., Douspis M., Dour M.L., 1999a, In: Banday et al. (1999), astro-ph/9810318
- Bartlett J.G., Douspis M., Blanchard A., Dour M.L., 1999b, *A&A*, submitted, astro-ph/9903045
- de Bernardis P., de Gasperis G., Masi S., Vittorio N., 1994, *ApJ*, 433, L1
- Bunn E.F., White M., 1997, *ApJ*, 480, 6
- Cheng E.S., Cottingham D.A., Fixsen D.J., et al., 1996, *ApJ*, 465, L71
- Devlin M., de Oliveira-Costa A., Herbig T., et al., 1998, *ApJ*, 509, L69
- Dicker S.R., Melhuish S.J., Davies R.D., et al., 1999, *MNRAS*, in press, astro-ph/9907118
- Eisenstein D.J., Hu W., Tegmark M., 1998, *ApJ*, 504, L57
- Eisenstein D.J., Hu W., Tegmark M., 1999a, In: Banday et al. (1999), astro-ph/9810318
- Eisenstein D.J., Hu W., Tegmark M., 1999b, *ApJ*, 518, 2
- Femenia B., Rebolo R., Gutierrez C.M., Limon M., Piccirillo L., 1998, *ApJ*, 498, 117

- Ganga K., Page L., Cheng E., Meyer S., 1994, *ApJ*, 432, L15
- Gundersen J.O., Line M., Staren J., et al., 1995, *ApJ*, 443, L57
- Hancock S., Gutierrez C.M., Davies R.D., et al., 1997, *MNRAS*, 289, 505
- Helbig P., 1999, *A&A*, 350, 1 (Paper III)
- Helbig P., Marlow D.R., Quast R., et al., 1999, *AAS*, 136, 297 (Paper II)
- Herbig T., de Oliveira-Costa A., Devlin M., et al., 1998, *ApJ*, 509, L73
- Leitch E.M., Readhead A.C.S., Pearson T.J., Myers S.T., Gulkis S., 1999, *ApJ*, in press, astro-ph/9807312
- Lineweaver C.H., 1998, *ApJ*, 505, L69 (L98)
- Lineweaver C.H., Barbosa D., Blanchard A., Bartlett J.G., 1997, *A&A*, 322, 365 (L97)
- Myers S.T., Rusin D., Marlow D., et al., 1999, in preparation
- Netterfield C.B., Devlin M.J., Jarosik N., Page L., Wollock E.J., 1997, *ApJ*, 474, 47
- de Oliveira-Costa A., Devlin M.J., Herbig T., et al., 1998, *ApJ*, 509, L77
- Platt S.R., Kovac J., Dragovan M., Peterson J.B., Rhul J.E., 1997, *ApJ*, 475, L1
- Quast R., Helbig P., 1999, *A&A*, 344, 721 (Paper I)
- Roos M., Harun-or-Rashid S.M., 1999, *A&A*, submitted, astro-ph/9901234
- Scott P.F., Saunders R., Pooley G., et al., 1996, *ApJ*, 461, L1
- Tanaka S.T., Clapp A.C., Devlin M.J., et al., 1996, *ApJ*, 468, L81
- Tegmark M., Hamilton A., 1997, In: A. V. Olinto J.A.F., Schramm D.N. (eds.), *Eighteenth Texas Symposium on Relativistic Astrophysics*, New York Academy of Sciences, New York, pp. 270–272, astro-ph/9702019
- Tegmark M., Eisenstein D.J., Hu W., 1998a, In: Thanh & Giraud-Heraud (1998), pp. 355–8, astro-ph/9804168
- Tegmark M., Eisenstein D.J., Hu W., Kron R.G., 1998b, *ApJ*, submitted, astro-ph/9805117
- Thanh J.T., Giraud-Heraud Y. (eds.), 1998, *Fundamental Parameters in Cosmology*, Proceedings of the XXXIIIrd Rencontres de Moriond, Paris, Éditions Frontiers
- Tucker G.S., Gush H.P., Halpern M., Shinkoda I., Towlson W., 1997, *ApJ*, 475, L73
- Turner M.S., 1999, In: Caldwell D.O. (ed.), *Particle Physics and the Universe (Cosmo-98)*, AIP, Woodbury, NY, astro-ph/9904051
- Webster A.M., Bridle S.L., Hobson M.P., et al., 1998, *ApJ*, 509, L65
- White M., 1998, *ApJ*, 506, 495
- White M., Scott D., 1996, *ApJ*, 459, 415
- White M., Srednicki M., 1995, *ApJ*, 443, 6
- Zaldarriaga M., 1998, *Fluctuations in the Cosmic Microwave Background*. Ph.D. thesis, Massachusetts Institute of Technology